ChemComm
Chemical Communications

Accepted Manuscript

This article can be cited before page numbers have been issued, to do this please use: I. Barlocco, S. Bellomi, B. M. C. Anghinelli, A. Villa, L. Prati, K. Föttinger, M. Stucchi, X. Chen and J. J. Delgado, *Chem. Commun.*, 2026, DOI: 10.1039/D5CC06925D.

ROYAL SOCIETY OF CHEMISTRY

rsc.li/chemcomm

ChemComm

View Article Online
DOI: 10.1039/D5CC06925D

COMMUNICATION

Influence of nitrogen functional groups in carbon-based support anchoring Pt nanoclusters and single atoms for efficient ammonia borane hydrolysis

Received 00th January 20xx,
Accepted 00th January 20xx

DOI: 10.1039/x0xx00000x

Ilaria Barlocco,[a] Silvio Bellomi,[b] Bianca M. C. Anghinelli,[a] Xiaowei Chen,[c] Juan J. Delgado,[c] Marta Stucchi,[a] Laura Prati,[a] Karin Föttinger[b] and Alberto Villa*[a]

Pt(II) precursor was impregnated onto graphite (C) and carbon nitride (CN_x), successfully forming subnanometric Pt clusters and single atoms. The N species on CN_x modified the electronic and topological structure of the metal, improving the catalytic properties of the Pt/CN_x catalyst in evolving hydrogen from NH_3BH_3. This was rationalised by combining HR-TEM and XPS characterisation with DFT computational analysis.

Supported noble-metal nanoparticles (MNPs) have been widely employed as catalysts in various sustainable chemical transformations, such as hydrogen production and biomass valorisation, due to their excellent activity and durability.[1]

It is well recognised that the catalytic properties of MNP-based catalysts are strongly dependent on their physicochemical properties, including structure, composition, shape, and size.[2] Indeed, the number and coordination of active sites are strictly correlated to the NP diameter, leading to a strong size-activity relationship where "every atom counts". Usually, the smaller the particle size, the higher the catalytic performance.[3] In this context, the support plays a fundamental role in tuning the properties of the metal phase. Indeed, MNPs and clusters deposited on different supports may display different reactivity.[4,5]

To this end, carbon materials are very attractive to support a variety of metal species. In fact, they are cheap, and their structure can be easily and finely tuned by introducing defects and heteroatoms.[6,7] Indeed, various electrocatalytic[8] and photocatalytic[9] studies have reported the possibility of obtaining outstanding catalytic properties in hydrogen production reactions by employing N-rich carbon materials as supports for sub-nanometric NPs.

In particular, in our previous work, we have shown exceptional activity, selectivity and stability in hydrogen production from hydrazine hydrate using Ir nanoclusters deposited on graphitic carbon nitride (GCN).[10] The increased catalytic features were ascribed to the N-containing moieties of GCN, causing electron density redistribution in the supported metal. Hu et al have anchored PtNi NPs on N-doped carbon nanotubes, demonstrating that the N-species accelerate the decomposition of hydrazine to ultra-pure hydrogen and stabilise the metal phase against agglomeration.[10]

Achieving efficient and safe hydrogen production is the key to move from traditional fossil fuels to "hydrogen energy".[11,12] Until now, different hydrogen storage materials have been developed to move this technology forward.

In this context, ammonia borane (AB) is a simple molecular hydride that can be used to produce hydrogen. Its hydrolytic dehydrogenation can be achieved under mild reaction conditions (room temperature and pressure) by means of a heterogeneous catalyst. In this reaction, water is not only the solvent, but also a hydrogen source, see Equation 1. Indeed, 3 moles of hydrogen can be released for one mole of AB.[13]

$NH_3BH_3 + 2H_2O \rightarrow NH_4BO_2 + 3H_2$ (g) (1)

The reaction involves the cleavage of B-H and O-H bonds in AB and H_2O molecules, respectively. Moreover, a catalyst needs to facilitate the transfer of the hydrogen atoms on the surface to evolve H_2.[14] To this end, Pt, Pd and Rh based catalysts were employed to rapidly and selectively decompose AB to molecular hydrogen.[15] In particular, it was shown that Pt sites can effectively activate and break B-H bonds.[16] Li and co-workers,[17] prepared Pt clusters of 1.2 nm embedded in a high surface area Co_3O_4 nanocage, and demonstrated that while the reducible oxide support can form $H^{\delta+}$ from H_2O, Pt clusters can accelerate the formation of $H^{\delta-}$ from AB.

It is in this context that this work finds application. Herein, we report the synthesis of Pt sub-nanometric clusters and single atoms supported on graphitic carbon material (graphite and carbon nitride). Pt(II) precursor was impregnated on the selected supports and reduced in-situ by means of the hydrogen produced from the AB decomposition. This allowed us to rationalise the catalytic properties of supported Pt on graphitic materials and unveil the role of N-functionalities. Indeed, despite having a similar structure, the materials differ for the

[a] Dipartimento di Chimica, Università degli Studi di Milano, via Golgi 19, I-20133 Milano, Italy. E-mail: alberto.villa@unimi.it
[b] Institute of Materials Chemistry, Technische Universität Wien, Getreidemarkt 9/165, Wien 1060 (Austria).
[c] Departamento de Ciencia de los Materiales, Ingeniería Metalúrgica y Química Inorgánica, Facultad de Ciencias, Universidad de Cádiz, Campus Río San Pedro, Puerto Real (Cádiz) E-11510, Spain.

† Electronic supplementary information (ESI) available.

View Article Online
DOI: 10.1039/D5CC06925D

intrinsic N content, profoundly modifying the electronic structure of carbon nitride with respect to graphite, and the subsequent interaction with Pt. To deeply understand the structure-activity relationship and metal-support interaction, the fresh and used catalysts were characterised by HR-TEM and XPS in combination with DFT, giving us an in-depth understanding of the enhanced catalytic properties shown by Pt/CN_x.

Commercial graphite (C) and synthesised carbon nitride (CN_x) were employed as supports for Pt clusters, with a loading of 1 wt%, prepared by the optimisation of the impregnation method proposed by Li and co-workers, and employing K_2PtCl_4 as metal precursor.[18] The obtained catalysts, Pt/CN_x and Pt/C, were then employed in the catalytic decomposition of ammonia borane (AB) near room temperature (303 K), with a catalyst : AB molar ratio of 1:1000. The pressure of evolved H_2, was elaborated to obtain the moles of hydrogen versus time. The kinetic profiles were evaluated for 100 minutes of reaction, where a plateau indicates the end of the AB decomposition for the most active catalyst, reaching the maximum volume of H_2 evolved, see Figure 1. Pt/C resulted to be nearly inactive reaching a maximum of $2.102 \cdot 10^{-1}$ mmol of H_2 produced, with a turn over frequency (TOF) of a 4.23 min^{-1}. An evaluation through 300 minutes of reaction did not reveal any change in the shape of the decomposition curve. Notably, passing from graphite to carbon nitride (Pt/CN_x), the moles of hydrogen evolved resulted to be $7.455 \cdot 10^{-1}$ mmol (almost four times more). Moreover, the TOF value increased to 6.36 min^{-1}. Because with this set-up the pressure observed is exclusively due to H_2 produced, we can assess that both catalysts are not capable to completely decompose AB. It is to be noted that the sigmoidal shape observed during the first reaction run in the evolution of H_2 can indicate the occurrence of structural changes during the reaction. This behaviour can be ascribed to a strong metal support interaction appearing only when Pt and N-functionalities are present. Indeed, in our previous study, we observed a similar trend for AB decomposition on $PtCo_3O_4$ catalyst, where the induction time was attributed to the transformation of the meta-stable active phase to a modified Pt species, following the Finke-Watzky kinetic model.[20] On the other hand, during stability tests (Figure S1), the disappearance of the induction period evidenced the stability of the in-situ formed active phase. After the fourth run, however, the catalyst showed a decreased initial activity, maintaining the same hydrogen productivity. This could be ascribed to the sintering of Pt small clusters, as confirmed from TEM (Figure 2j-l).

XPS was performed to correlate the information gained by catalysis with the sample surface composition. The results of the survey analysis are summarised in Table S1. We could observe a Pt exposure of only 0.10 % for Pt/C, four times less than on Pt/CN_x (0.39 %), despite the similar content of the bulk measured by ICP. The narrow scans of the Pt4f signals, as well as C 1s and N 1s were fitted using the model described in the ESI (Figure 2b, S2-3).

The fresh catalysts presented almost uniquely surface Pt^{II}: 99.8 % for Pt/C and 89.8 % for Pt/CN_x, in agreement with the nature of the precursor (K_2PtCl_6), and confirmed from the presence of Cl 2p peak.

On Pt/CN_x, after the reaction, Pt^{II} is reduced to metallic Pt (59.6 % of Pt^0), the amount of surface Pt remained almost constant

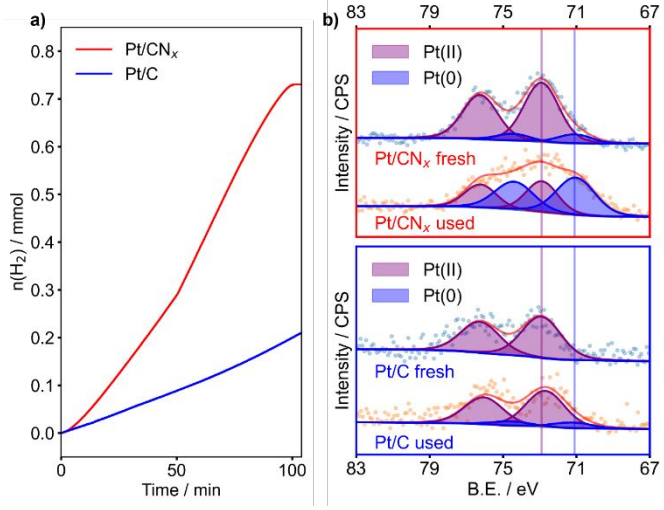

Fig. 1 a) kinetic profiles of hydrogen evolution rate of Pt/C (blue) and Pt/CN_x (red). b) XPS of Pt/CN_x (upper panel) and Pt/C (lower panel), fresh and used.

(0.35 %), but the Cl 2p peak was completely removed. The high content of oxidised species is consistent with a strong electronic interaction with the support.[19] Indeed, the ratio between the C-N-C and the C=C signal of the CN_x support decreased from 1.2 to 1.1, and the C-N-C peak shifted negatively by 0.2 eV (Figure S2 and Table S3), indicating a higher coverage of the N functionalities on the spent catalyst.[19] This was confirmed by the decrease of the relative percentage of the quaternary N from 8.4 to 7.2 % (Figure S3 and Table S4). On the other hand, in the used Pt/C, Pt was mostly observed as Pt^{II} (13.7 % of Pt^0), although the disappearance of Cl 2p peak indicated the decomposition of the precursor. The overall amount of Pt decreased (0.06 wt%), suggesting agglomeration of the particles. No significant change was observed from the C 1s signal at the resolution available from the instrument employed. For both catalysts, the lack of any distinguishable B 1s and B KLL peaks was taken as an evidence of the absence of residual borates poisoning the active site.[15]

Overall, the XPS analyses corroborate the catalytic test results: the CN_x support, through its nitrogen functionalities, promotes a strong metal-support interaction that forms and stabilises the Pt active phase during reaction, an effect not observed with the graphite support.

Therefore, the morphology of the fresh materials was investigated with TEM to examine the size and dispersion of Pt clusters on the two supports used: graphite and carbon nitride. Figure 2 shows representative STEM-HAADF images of the Pt catalysts in their fresh state, as well as the particle size distribution. We could observe that on both fresh Pt/C and Pt/CN_x, the clusters are homogeneously distributed on the surfaces, indicating a good dispersion. It should be emphasised that it was impossible to measure the nanoclusters smaller than 0.5 nm, as shown in Figure 2b. Excluding nanoparticles smaller

View Article Online
DOI: 10.1039/D5CC06935D

than 0.5 nm, the average particle size on Pt/C was 1.7 nm. Most particles fall within the 0.5 to 2.0 nm range, although a few larger particles exceeding 4 nm were observed on the Pt/C catalyst.

Fig. 2 STEM-HAADF images of (a-b) fresh Pt/C, (d-e) used Pt/C, (g-h) fresh Pt/CN_x and (j-k) used Pt/CN_x catalysts. Particle size distribution of (c) fresh Pt/C, (f) used Pt/C, i) fresh Pt/CN_x and (l) used Pt/CN_x catalysts.

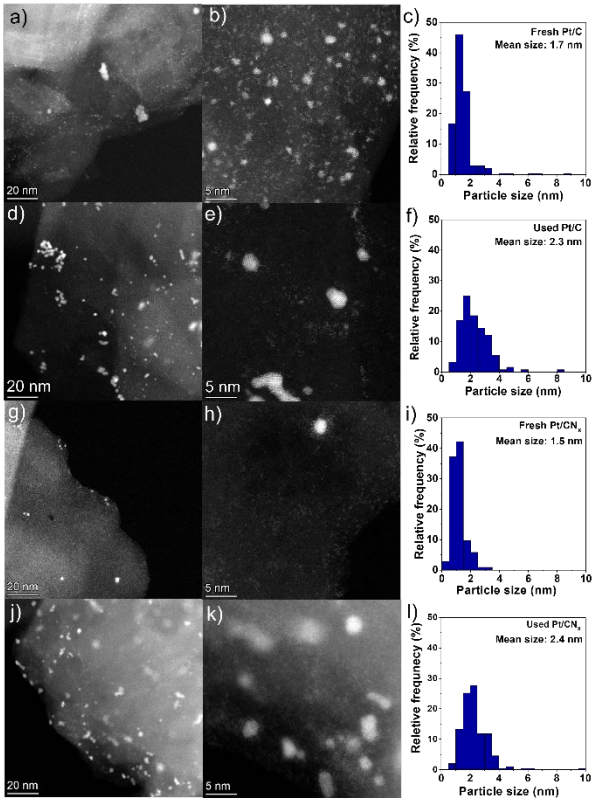

However, a few Pt particles on the Pt/C catalyst exceeded 4 nm. In contrast, the particle sizes on the Pt/CN_x catalyst were all below 3.5 nm and displayed a more uniform distribution. The average particle size was 1.5 nm, without counting very small clusters below 0.5 nm and single atoms (Figure 2h). This could be attributed to the unique structure of the carbon nitride support, which effectively stabilized both very small clusters and individual metal atoms.[20,21]

The results were corroborated by XRD. For the Pt/CN_x sample, the diffractograms of bare CN_x and the catalysts showed the same two peaks, i.e. 2θ of 13.4° and 27.2° attributed to (100) and (002) planes of carbon nitride, respectively (Figure S4).[22] The absence of Pt-related peaks indicates the presence of small Pt clusters. Comparing the TEM images of both fresh Pt catalysts with the used, an increase of the mean particle size was observed, from 1.7 nm to 2.3 for the Pt/C catalyst and from 1.5 nm to 2.4 nm for the Pt/CN_x catalyst, as shown in the right column of Figure 2. Although small nanoclusters and single atoms were still present in both the used Pt/C and Pt/CN_x catalysts, Pt nanoparticles larger than 4 nm were also observed. In addition, the fraction of nanoparticles smaller than 2 nm in both used catalysts is significantly lower than in the fresh catalysts. This could be ascribed to the coalescence of the small clusters during the substrate decomposition to partially form nanoparticles, confirming the transition to another metal phase during the reaction.

To gain a deeper understanding of the metal-support interaction of Pt nanostructures deposited on carbon nitride and to study the enhanced catalytic behaviour of Pt/CN_x with respect to Pt/C, DFT analysis was performed.

The results of the simulations are presented in Figure 3 and Table 1. Firstly, pristine graphene (PG) was selected as a model for graphite, and the corrugated carbon nitride structure (CN) characterised by heptazine pores represented CN_x.[23] Next, an eight atoms Pt cluster was optimised on PG and CN (see ESI for the detailed global optimisation procedure). The cluster adsorption on the two different supports was evaluated in terms of adsorption (E_{ads}), adhesion (E_{adh}) and deformation (E_{def}) energies, Table 1, as previously reported.[19] Indeed, Pt_8 cluster was more strongly anchored on carbon nitride than on graphene, demonstrating an enhanced interaction for Pt_8/CN. Then, an analysis of the charge transfer between the support and the Pt cluster was performed to elucidate its influence on the structure-activity relationship. We observed a net charge redistribution when carbon nitride is the support. In fact, a gain of electron density on the top of the cluster (yellow) and depletion at the interface (blue) was noticed, supporting the superior reactivity due to MSI.

Tab. 1 Energetic and structural information of Pt_8 cluster interacting with the supports. Adsorption energy (E_{ads}), adhesion energy (E_{adh}), deformation energy (E_{def}), platinum-carbon distance (d Pt-C), platinum-nitrogen distance (d Pt-N), and the maximum and the minimum distances between platinum atoms in the cluster (d_{max} Pt-Pt and d_{min} Pt-Pt, respectively) are reported.

Structure	E_{ads} /eV	E_{adh} /eV	E_{def} /eV	$\bar{d}$ Pt-C /Å	$\bar{d}$ Pt-N /Å	d_{max} Pt-Pt /Å	d_{min} Pt-Pt /Å
Pt/PG	-2.97	-3.11	-0.14	2.29	-	2.69	2.43
Pt/CN	-3.76	-4.32	-0.56	2.19	2.05	2.66	2.44

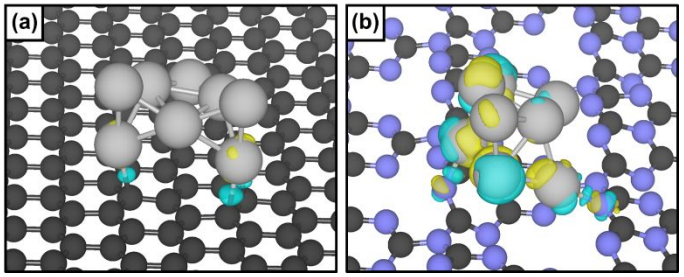

Fig. 3 Charge density difference plot of (a) Pt_8/PG and (b) Pt_8/CN. Carbon atoms are represented in black, nitrogen in light blue and platinum in grey. Yellow and blue iso-surfaces denote gain and depletion of electron density respectively, and the iso-surface value is $9 \cdot 10^{-3}$ e^{-} $Å^{-2}$.

In conclusion, in this work, a combination of experimental and computational approaches was employed to elucidate the role of N-functionalities in carbon materials in enhancing the reactivity toward the hydrolytic decomposition of ammonia borane. Two catalysts, Pt/C and Pt/CN_x, were prepared *via* a modified wet impregnation method. The nitrogen species in CN_x significantly altered the electronic and structural properties of the support, thereby improving the catalytic performance of Pt/CN_x in hydrogen evolution from ammonia borane.

View Article Online
DOI: 10.1039/D5CC06925D

Interestingly, the Pt/CN_x catalyst exhibited a sigmoidal hydrogen evolution profile, indicative of a transition from a metastable active species to a more stable one. XPS and TEM analyses revealed that the enhanced activity of Pt on carbon nitride arises from a greater exposure of surface metal species. Moreover, the evolution of the active phase under reaction conditions was corroborated by particle growth due to coalescence and by partial Pt reduction in the used catalyst.

DFT calculations were performed to model Pt_8/PG and Pt_8/CN systems, representing Pt/C and Pt/ CN_x, respectively. A stronger interaction between the Pt_8 cluster and the carbon nitride support was observed, accompanied by charge redistribution within the cluster, accounting for the superior reactivity and metal-support interaction.

The combined experimental and theoretical study highlights that the enhanced catalytic properties of Pt/CN_x originate from a strong metal-support interaction due to the presence of N-functionalities, providing a coherent explanation for the observed reactivity and characterisation results.

Conflicts of interest

There are no conflicts to declare.

Data availability

The data supporting this article have been included as part of the Supplementary Information.

Acknowledgements

This work has been partially supported by the project PID2023-149274NB-I00, funded by MICIU/AEI/10.13039/501100011033 and co-funded by the European Regional Development Fund (ERDF) -"A way of making Europe".

This research was funded in part by the Austrian Science Fund (FWF) 10.55776/F8100. For open access purposes, the author has applied a CC BY public copyright license to any author accepted manuscript version arising from this submission. We acknowledge the Analytical Instrumentation Center (AIC) at TU Wien for the analysis time.

The Italian Ministry of Environment and Energy Sustainability (MASE, formerly MITE) is gratefully acknowledged for funding the project "RSH2A_000018 - Stoccaggio e distribuzione di idrogeno attraverso una strategia power-to-gas/gas-to-power con cattura ed utilizzo completi del carbonio - Hydrogen storage and distribution through power-to-gas strategy, with full carbon capture and utilization" (CUP: F57G25000180006) in the frame the European Union Next-GenerationEU, Piano Nazionale di Ripresa e Resilienza (PNRR) – Missione 2 "Rivoluzione verde e transizione ecologica", Componente 2 "Energia rinnovabile, idrogeno, rete e mobilità sostenibile", Investimento 3.5 "Ricerca e sviluppo sull'idrogeno" (M2C2I3.5, bando A).

Notes and references

1 E. Gianotti, M. Taillades-Jacquin, J. Rozière and D. J. Jones, *ACS Catal*, 2018, 8, 4660–4680.
2 T. S. Rodrigues, A. G. M. da Silva and P. H. C. Camargo, *J Mater Chem A Mater*, 2019, 7, 5857–5874.
3 M. Haruta, T. Kobayashi, H. Sano and N. Yamada, *Chem Lett*, 1987, 16, 405–408.
4 M. Haruta, *Catal Today*, 1997, 36, 153–166.
5 S. Bonanni, K. Aït-Mansour, W. Harbich and H. Brune, *J Am Chem Soc*, 2012, 134, 3445–3450.
6 M. S. Shafeeyan, W. M. A. W. Daud, A. Houshmand and A. Shamiri, *J Anal Appl Pyrolysis*, 2010, 89, 143–151.
7 H. Yu, F. Peng, J. Tan, X. Hu, H. Wang, J. Yang and W. Zheng, *Angewandte Chemie - International Edition*, 2011, 50, 3978–3982.
8 Y. Jiao, Y. Zheng, K. Davey and S.-Z. Qiao, *Nat Energy*, 2016, 1, 16130.
9 R. Sharma, M. Almáši, S. P. Nehra, V. S. Rao, P. Panchal, D. R. Paul, I. P. Jain and A. Sharma, *Renewable and Sustainable Energy Reviews*, 2022, 168, 112776.
10 X. Hu, T. Liu, X. Zhang and J. Tian, *Chemical Communications*, 2021, 57, 8324–8327.
11 L. Schlapbach and A. Züttel, *Nature*, 2001, 414, 353–358.
12 S. Singh, S. Jain, V. PS, A. K. Tiwari, M. R. Nouni, J. K. Pandey and S. Goel, *Renewable and Sustainable Energy Reviews*, 2015, 51, 623–633.
13 C. D. Mboyi, D. Poinsot, J. Roger, K. Fajerwerg, M. L. Kahn and J.-C. Hierso, *Small*, 2021, 17, 2102759.
14 S. Guan, Z. Yuan, S. Zhao, Z. Zhuang, H. Zhang, R. Shen, Y. Fan, B. Li, D. Wang and B. Liu, *Angewandte Chemie*, DOI:10.1002/ange.202408193.
15 S. Bellomi, D. C. Cano-Blanco, Y. Han, J. J. Delgado, X. Chen, K. A. Lomachenko, I. Barlocco, D. Ferri, A. Roldan and A. Villa, *Appl Surf Sci*, 2025, 711, 164116.
16 J. Jiang, J. Zhang, B. Wu and S. Tu, *J Alloys Compd*, 2023, 969, 172369.
17 M. Li, S. Zhang, J. Zhao and H. Wang, *ACS Appl Mater Interfaces*, 2021, 13, 57362–57371.
18 Y.-T. Li, X.-L. Zhang, Z.-K. Peng, P. Liu and X.-C. Zheng, *ACS Sustain Chem Eng*, 2020, 8, 8458–8468.
19 S. Bellomi, I. Barlocco, X. Chen, J. J. Delgado, R. Arrigo, N. Dimitratos, A. Roldan and A. Villa, *Physical Chemistry Chemical Physics*, 2023, 25, 1081–1095.

View Article Online
DOI: 10.1039/D5CC06925D

20I. F. Teixeira, E. C. M. Barbosa, S. C. E. Tsang and P. H. C. Camargo, *Chem Soc Rev*, 2018, 47, 7783–7817.
21Y. Li, T. Kong and S. Shen, *Small*, DOI:10.1002/smll.201900772.
22M. Ismael, Y. Wu, D. H. Taffa, P. Bottke and M. Wark, *New Journal of Chemistry*, 2019, 43, 6909–6920.
23I. Barlocco, L. A. Cipriano, G. Di Liberto and G. Pacchioni, *J Catal*, 2023, 417, 351–359.

View Article Online
DOI: 10.1039/D5CC06925D

Data availability

The data supporting this article have been included as part of the Supplementary Information.